ACS APPLIED MATERIALS & INTERFACES

Research Article

www.acsami.org

Graphene Oxide–Phosphor Hybrid Nanoscrolls with High Luminescent Quantum Yield: Synthesis, Structural, and X-ray Absorption Studies

Janardhanan R. Rani,[†] Se-I Oh,[†] Jeong Min Woo,[†] Nilesh L. Tarwal,[†] Hyun-Woong Kim,[†] Bongjin Simon Mun,[‡] Sungbae Lee,[‡] Ki-Jeong Kim,[§] and Jae-Hyung Jang*[,†]

[†]School of Information and Communications and [‡]Ertl Center for Electrochemistry and Catalysis, Department of Physics and Photon Science, Gwangju Institute of Science and Technology, Gwangju 500-712, South Korea

[§]Beamline Research Division, Pohang Accelerator Laboratory, Pohang, Kyungbuk 790-784, South Korea

Supporting Information

ABSTRACT: Highly luminescent graphene oxide (GO)–phosphor hybrid thin films with a maximum quantum yield of 9.6% were synthesized via a simple chemical method. An intense luminescence emission peak at 537 nm and a broad emission peak at 400 nm were observed from the GO–phosphor hybrid films. The maximum quantum yield of the emissions from the hybrid films was found to be 9.6%, which is 48 times higher than that of pristine GO films. The GO–phosphor hybrids were prepared via spin-coating and subsequent postannealing of the films, resulting in scrolling of the GO sheets. The resulting GO nanoscrolls exhibited a length of ~2 μm with nanoscale interior cavities. Transmission electron microscopy and selected-area electron diffraction analyses revealed that the lattice structure of the tubular scrolls is similar to that of carbon nanotubes. While pristine GO films are p-type, in the GO–phosphor hybrids, the Fermi level shifted upward and fell between the HOMO–LUMO gap due to phosphor attachment via C–N bonding. The highly luminescent GO–phosphor hybrids will find important applications in graphene-based optoelectronic devices.

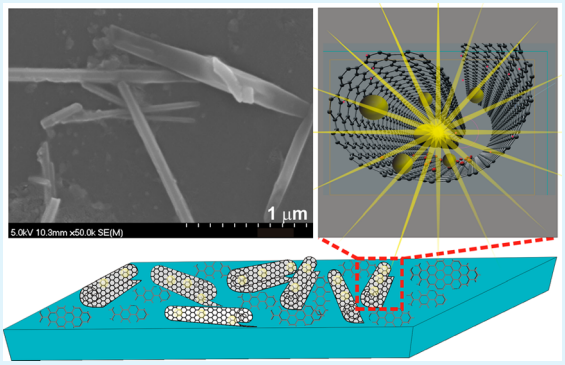

KEYWORDS: *graphene oxide, nanoscrolls, carbon nanotubes, X-ray absorption*

1. INTRODUCTION

Graphene, a single-atom-thick sheet of hexagonally arrayed sp^2-bonded carbon atoms, has received significant attention due to its unique electronic, mechanical, and thermal properties, which originate from its semimetallic nature and linear electronic band structure.[1−3] Many potential applications of graphene in optoelectronic devices such as lasers and light-emitting diodes have been hindered, however, by the zero optical bandgap of the Dirac cone. Nevertheless, graphene and its derivatives offer significant advantages such as low toxicity, good biocompatibility, and chemical inertness. The development of highly efficient luminescent graphene or graphene derivatives is thus technologically important for optoelectronic device applications. However, the quantum yield of photoluminescence from graphene lies in a range from 1×10^{-12} to 1×10^{-9}, which is too low for practical applications. Tremendous efforts have been made to enhance the quantum yield of photoluminescence from graphene, including the introduction of defects or modification of its carbon network with oxygen-bearing functional groups.[4,5]

Converting graphene into graphene oxide (GO) is one of the feasible solutions for the generation of luminescence in graphene. In contrast to pristine graphene in which all atoms are sp^2 hybridized, GO consists of sp^3 carbon atoms covalently bonded to oxygen-bearing functional groups, which results in a finite electronic bandgap generated by the disruption of π-networks. Controlling the ratio of sp^2/sp^3 thus opens up possibilities of the bandgap engineering of graphene-related materials. Commonly used oxidation methods result in the oxidation of sp^2 surfaces and the periphery of the graphene sheet. This surface oxidation generates many defects, which in turn reduce the luminescence efficiency of GO. Therefore, even with a finite bandgap, GO films typically exhibit weak luminescence and low quantum yield (0.02 to 0.2%), which limit their application in optoelectronic devices.

For practical optoelectronic device applications, it is necessary to modify GO to achieve stronger and more efficient visible photoluminescence. Various methods investigated to promote light emission efficiency of GO solutions include the functionalization of graphene using nitrogen groups, the application of reduction treatments, passivation of surface reactive sites by amide formation, etc.[6−8] These processes,

Received: October 23, 2014
Accepted: February 24, 2015
Published: February 24, 2015

DOI: 10.1021/am507342w
ACS Appl. Mater. Interfaces 2015, 7, 5693−5700

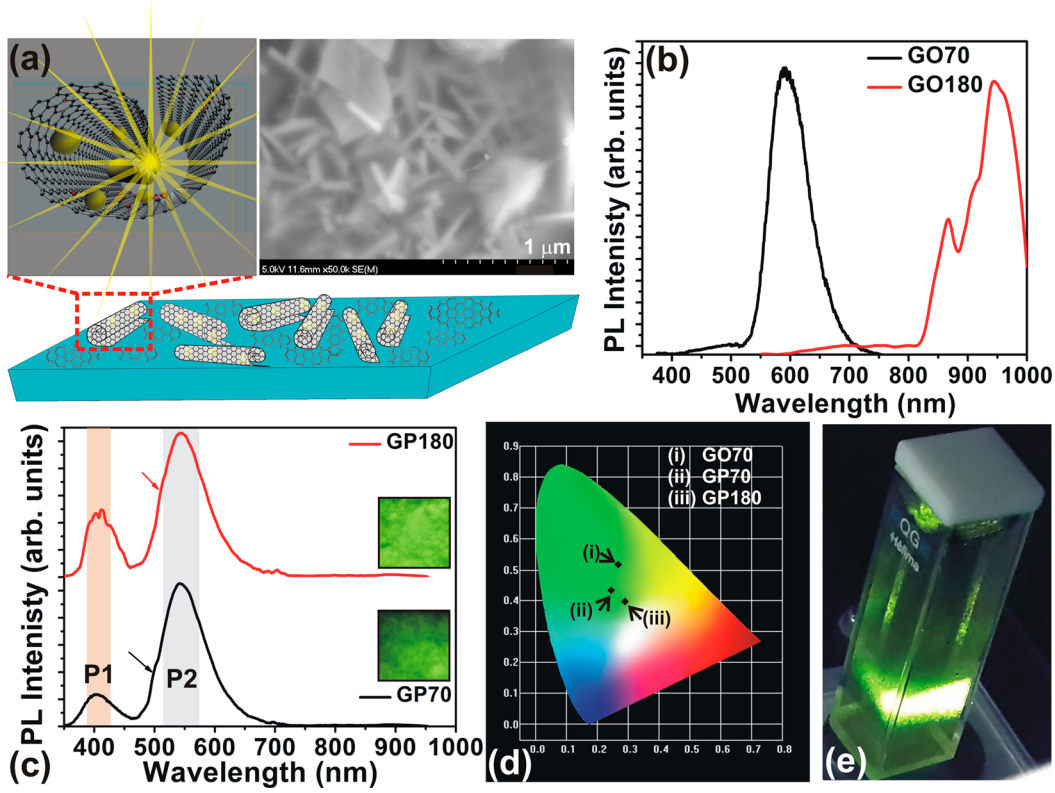

Figure 1. (a) SEM image and schematic showing the GO−phosphor hybrid nanoscrolls in GP180, PL emission spectra of (b) GO70 and GO180 films, (c) GP70 and GP180 films measured with an excitation wavelength of 280 nm. (d) CIE chromaticity coordinates of the PL emission from the synthesized thin films and (e) digital image of the strong PL emission from the GO−phosphor hybrid solution.

however, involve several steps and are time-consuming. Moreover, these modifications have not resulted in the desired enhancement of quantum yield. It is therefore necessary to develop GO-based hybrid materials that preserve the unique properties of GO while enhancing luminescent efficiency.

Inorganic phosphors that can emit visible light are suitable candidates for synthesizing such hybrid materials. These phosphors have high quantum yields and can be embedded in GO sheets to produce GO−phosphor hybrids with improved light-emission efficiency. The GO−phosphor hybrids combine the unique advantage of luminescent emission from phosphor with the superior physical and chemical properties of GO. Additionally, attaching a heavy phosphor to the GO will convert the GO sheets to GO−phosphor nanoscrolls.

Graphene nanoscrolls (GNS) and GO nanoscrolls (GONS), formed by rolling graphene or GO layers, respectively, in one or more directions, are new members of the graphene family. Embedding phosphor particles into graphene oxide sheets results in the formation of GO−phosphor hybrid nanoscrolls that have the unique characteristics of graphene with high luminescence efficiency. Such GNS/GONS have additional advantages. Graphene is known to undergo large out-of-plane thermal fluctuations, and its free edges make it susceptible to edge defects, whereas GNS/GONS, with closed edges, retains the high conductance and excellent transport properties of graphene/GO.[9]

Herein, we report the synthesis and characterization of GO−oxynitride phosphor hybrids via a simple chemical process. The fabricated hybrids exhibited enhanced luminescence that is suitable for optoelectronic device applications. Furthermore, it was found that annealing of the GO−phosphor hybrid structure results in the formation of nanoscrolls. Structural and optical properties of the GO−phosphor nanoscrolls were characterized and analyzed. The quantum yield of photoluminescence (PL) emissions from thin films of the GO−phosphor nanoscrolls was found to be 48 times higher than that of pristine GO films. To the best of our knowledge, the quantum yield is the highest reported to date for GO thin films. The findings of this study demonstrate that the synthesis of GO−phosphor hybrids opens the possibility of fabricating highly efficient optoelectronic devices.

2. EXPERIMENTAL DETAILS

GO was synthesized by a modified Hummers method[10] to give a dispersion of GO under ultrasonication. The $SrBaSi_2O_2N_2:Eu^{2+}$ phosphor material was embedded in a GO solution via a simple chemical process. The GO solution (6 mL, concentration 0.3 mg/mL) and phosphor colloid solution (4 mL, concentration 0.1 mg/mL) were separately sonicated in deionized water for 30 min and mixed together. Then, the mixture was further sonicated for 10 min, and the resulting GO−phosphor hybrid solution was spin-coated on a Si substrate covered with a 300 nm thick SiO_2 layer. The substrates were successively cleaned using distilled water and acetone in an ultrasonic cleaner for 30 min. Typically, the substrate was completely covered with a sufficient amount of the GO−phosphor solution. Then the GO−phosphor hybrid solution was spin-coated multiple times at 500, 800, and 1600 rpm for 30 s for each speed of rotation and was subsequently annealed at various temperatures using a hot plate. On the basis of their compositions and annealing temperatures, the films were named as GO70 (GO film annealed at 70 °C), GO180 (GO film annealed at 180 °C), GP70 (GO−phosphor hybrid film annealed at 70 °C), and GP180 (GO−phosphor hybrid film annealed at 180 °C).

The structural and optical properties of the films were investigated by scanning electron microscopy (SEM) (JEOL, JSM-6700F), Raman

DOI: 10.1021/am507342w
ACS Appl. Mater. Interfaces 2015, 7, 5693−5700

Table 1. Fitting Parameters and the Corresponding Peak Assignments of the C 1s and N 1s XPS Spectra of the GO70, GO180, GP70, and GP180 Films

	C 1s				N 1s		
sample	B.E (eV)	assignment	ref	sample	B.E (eV)	assignment	ref
GO70/GO180	284.8	sp^2 carbon	13	phosphor	395.2	N−H	14
	286.9	O−H/O−C−O	13		396.89	N−H	14
	288.9	O−C═O	13		397.95	Si_3N	14
					398.4	Si_3N_4	14
					399. 17	NSi_2O	14
GP70	284.1	sp^2 carbon	13	GP70	394.5	N−H	14
	285.6	C−N	15		396.42	N−H	14
	286.7	O−H/O−C−O	13		398.2	Si_3N_4	14
	288.2	N−C═O	15		399.47	NSi_2O	16
	290. 1	O−C (: O)−N	15		400.25	C−N═O	17
	291.2	C attached to nitroxyl group	18		401.5	oxidized nitrogen	17
GP180	284.1	sp^2 carbon	13	GP180	394.5	N−H	14
	285.6	C−N	15		396.2	N−H	14
	286.7	O−H/O−C−O	13		397.4	Si_3N	14
	288.2	N−C═O	15		398.8	Si_3N_4	14
	290.15	O−C (: O)−N	15		400	C═N	17

spectroscopy (in via Raman microscope), UV−visible absorption studies (JASCO V-650), X-ray diffraction (XRD) (Rigaku-D/MAX-2500H), high-resolution transmission electron microscopy (HRTEM)/selected area electron diffraction (SAED)/energy dispersive X-ray (EDX) spectral (JEM.ARM.200F) analyses, and photoluminescence (PL) (PerkinElmer-LS 55) measurements. For the SEM analysis, films deposited on a Si substrate were coated with Pt prior to measurement. For HRTEM and SAED measurements, the films were deposited onto carbon-coated Cu grids and annealed at 70 and 180 °C, respectively. The quantum yield of the PL emission was measured using the absolute PL quantum yield measurement system (model: Biorad/C10027/C9920−20, Hamamatsu). For the absorption and quantum yield measurements, films were deposited on quartz substrates. The measurements of ultraviolet and X-ray photoemission spectroscopy (UPS/XPS) were carried out at beamline 8A2 of the Pohang Accelerator Laboratory (PAL) using a synchrotron radiation source. A hemispherical electron analyzer, Scienta 100, was used to obtain the XPS/UPS spectra. The cyclic voltammograms of the films were measured using a standard three-electrode cell that has counter and reference electrodes made with a Pt wire and a standard Ag/AgCl, respectively. An aqueous solution of 0.1 M phosphate buffer saline (PBS) was used as the electrolyte in all electrochemical experiments. Cyclic voltammograms in a range of −1.6 to 1.6 V were taken at a scan rate of 10 mV/s for all the samples using a computerized potentiostat−galvanostat.

3. RESULTS AND DISCUSSION

The formation of GONS was confirmed by SEM. The SEM image and a schematic showing the GO−phosphor hybrid nanoscrolls in GP180 are shown in Figure 1a. The PL emission spectra from the films are shown in Figure 1b,c. Figure 1b shows the PL emission spectra of the GO70 and GO180 films, and Figure 1c shows the PL emission spectra of the GP70 and GP180 films. GO possesses a finite bandgap generated by the disruption of π networks due to the formation of oxygen functional groups. PL emission thus takes place from the transition between $\pi-\pi^*$ energy gaps. The GO70 film produces emissions at ∼590 nm with a $\pi-\pi^*$ gap of ∼2.05 eV, while the GO180 film shows a peak at ∼950 nm with a $\pi-\pi^*$ gap of ∼1.3 eV. The GP70 and GP180 films show a broad emission at ∼400 nm (P1 in Figure 1c) and an intense peak at ∼537 nm (P2 in Figure 1c). The 537 nm peak in the GP70 and GP180 films is from the $4f^6 5d \rightarrow 4f^7$ transitions in Eu^{2+} of the phosphor.[11,12] The GO−phosphor hybrid films show shoulder peaks at ∼500 nm (for GP70) and 510 nm (for GP180), which correspond to $\pi-\pi^*$ gap values of ∼2.56 and 2.43 eV, respectively. The origin of these emission peaks from the GO−phosphor hybrid films is discussed later. Very intense PL emissions were observed from the GP70 and GP180 films as shown in the inset of Figure 1c. The 1931 CIE chromaticity coordinates of the PL emission from the synthesized thin films are shown in Figure 1d. The CIE coordinates show that the GO70 film exhibits an emission in the green region, while it shifts toward the white region for the GP180 film. The shift toward the white region is due to the emission from both GO and phosphor. Figure 1e shows a digital image verifying the intense PL emission from the GO−phosphor hybrid solution (in a quartz cuvette) when it is excited by 280 nm light. This solution was used to prepare the GO−phosphor thin films such as GP70 and GP180.

To analyze the nature of bonding between GO and phosphor particles, XPS analysis was carried out. The incident photon energy was set to 630 eV to obtain the C 1s and N 1s XPS spectra. The C 1s and N 1s spectra were deconvoluted into several peaks, and the assignments of peaks are shown in Table 1.

The C 1s XPS spectra of the films, shown in Figure 2a, clearly indicate considerable degree of oxidation of carbon, which corresponds to the addition of various functional groups.[13] The relative intensity of the O−H/O−C−O and O−C═O peaks decreases in GO180 compared to GO70, which is presumably due to the reduction of GO during annealing process. In the GP70 and GP180 films, the peak observed at ∼285.5 eV corresponds to C−N bonding. The peak at ∼288.9 eV (O−C═O) observed in the GO70 and GO180 films shifts to 288.2 eV in the GP70 and GP180 films. This peak observed at 288.2 eV corresponds to N−C═O bonding. The peak at ∼290.1 eV is due to O−C (: O)−N, and the peak at ∼291.2 eV corresponds to carbon atoms attached to nitroxyl groups.[18] When the spectra of the GP70 and GP180 films are compared, the intensity of the 290.1 eV peak (O−C(:O)−N) decreases, and the 291.2 eV (carbon−nitroxyl) peak is absent in the GP180 film. Also, an increased in intensity of the 285.6 eV (C−N) peak in GP180 film, indicates that carbon in the GO is connected to the relatively heavy phosphor

DOI: 10.1021/am507342w
ACS Appl. Mater. Interfaces 2015, 7, 5693−5700

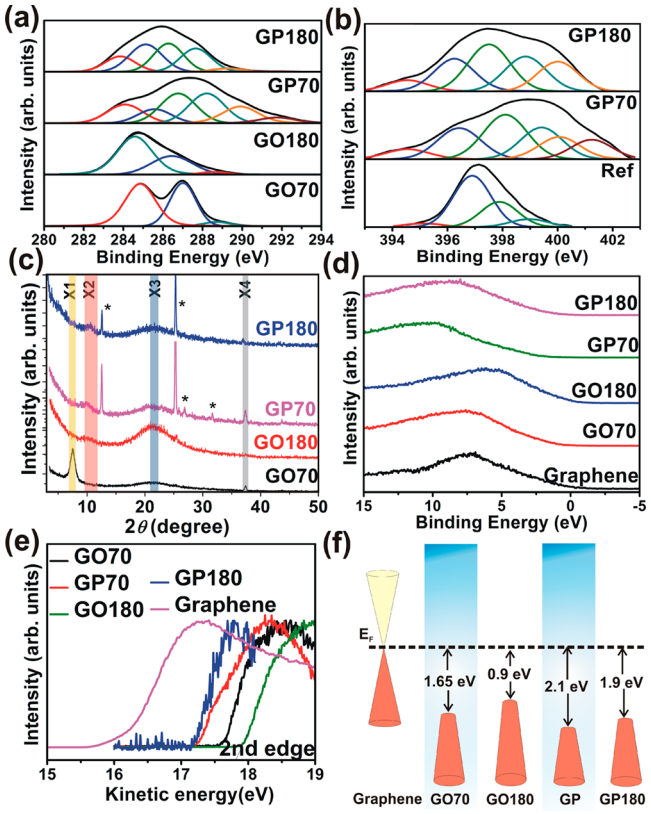

Figure 2. (a) C 1s and (b) N 1s XPS spectra of the deposited films, (c) XRD spectra of the films (* peaks are from the phosphor), (d) valence-band UPS spectra measured with a photon energy of 130 eV, and (e) kinetic energy cutoff of the secondary electron with a photon energy of 130 eV, (f) schematic representation of the HOMO position with respect to E_F.

via nitrogen, which results in scrolling. In the GP70 films, the supplied external thermal energy was not sufficient to form strong C−N bonding, which prevented complete scrolling of the GO sheets. From the XPS analysis, the carbon-to-oxygen ratios (C/O) of GO70, GO180, GP70, and GP180 were found to be 0.17, 0.92, 1.16, and 1.5, respectively. It suggests that reduction occurred during the phosphor embedding and annealing processes.

The high-resolution N 1s spectra are shown in Figure 2b, and the assignments of the deconvoluted peaks are provided in Table 1. In comparison with the N 1s XPS peaks of GP70 film, the peaks of the GP180 films are shifted to lower binding energy. The peak observed in GP180 at ∼400 eV can be ascribed to C═N bonding.[16] It is worth noting that peaks observed in GP70 at 400.25 eV (corresponding to (C−N═O)) and 401.5 eV (assigned to oxidized nitrogen) are absent in the GP180 film. This further confirms that, in the GP70 and GP180 films, phosphor molecules were attached with graphene via C−N bonding, and the bonding is more prominent in the latter due to annealing at a higher temperature. These are consistent with those observed from the C 1s XPS spectra. The scrolling of GO sheets in the GP180 film is thus due to graphene−phosphor attachment via nitrogen during the annealing process. The Si 2p and O 1s XPS spectra of all the films are shown in Supplementary Information, Figure S1.

The variations in the degree of oxidation in the films were confirmed through XRD analysis. The increase in interplanar spacing in the lattice is a direct measure of the degree of oxidation in graphene. The XRD spectra of the films in Figure 2c show a broad diffraction peak at $2\theta = 22.30°$, (X3 in Figure 2c) due to the short-range order in the stacked GO sheets.[19] The typical diffraction peak of native graphite is observed at $\sim 2\theta = 26.30°$ ($d = 0.34$ nm). In our films, the diffraction peak observed at $2\theta = 22.30°$ represents a typical reduced GO film, and it corresponds to a layer-to-layer distance (d-spacing) of ∼0.38 nm. In the GO70 film, the peak observed at $\sim 2\theta = 7.5°$ (X1 in Figure 2c) indicates a higher degree of oxidation during the film growth. This X1 peak shifts to $2\theta = 10.26°$, in the GO180, GP70, and GP180 films (marked as X2 in Figure 2c) with reduced intensity. This shift from X1 to X2, which was observed in GO180 film, occurs due to the reduction of GO via annealing of the films at higher temperature, while the corresponding shift observed in GP films occurred due to the phosphor embedding in GO sheets. Moreover, the shift from X1 to X2 in GO180, GP70, and GP180 films also indicates less degree of oxidation, compared to the GO70 film. The increased intensity of the X3 peak in the GO180 film clearly indicates that annealing at 180 °C results in the formation of more sp^2 clusters. The intensity of the X2 peak in the GP70 film is lower than that of the X1 peak in the GO70 film, while the intensity of the X3 peak remains the same, which is presumably due to the conversion of C−O bonding to C−N bonding. The XRD analysis confirms the variation in degree of oxidation in all the films and the presence of a C−N bonding in GP films, which is consistent with the observations from XPS analysis.

To analyze the origin of PL emission in the GO−phosphor hybrid film, a detailed study of the structural variations and electronic structures of the films was carried out using valence-band UPS (Figure 2d). The UPS spectra were measured with the photon energy of 130 eV. The valence-band electrons responsible for bonding are the fingerprint of the structural changes. A peak at ∼11 eV corresponds to s−p mixed hybridized state electrons in the GO70 film. This peak shifts to 9.5 eV in the GO180 film (a 1.5 eV binding energy difference),[16] which is due to the generation of more C $2\pi-\pi$ electrons via annealing. A peak appears at 13.8 eV in the GP70 film due to the contribution of both carbon and nitrogen electrons (C 2p and N 2p electrons shared through σ bonds).[20] The peak observed at 13.8 eV in GP70 film shifts to 12.3 eV in the GP180 film due to the annealing process.

The work function values are calculated from the valence-band secondary electron emission edge spectra in Figure 2e. The work function values of the samples were measured as the difference between the kinetic energy cutoff (E_{cutoff}) of the secondary electrons and the Fermi level (E_F).[21] The work function values were found to be 4.1, 6.2, 5.8, 5.5, and 5.3 eV for pure graphene, GO70, GO180, GP70, and GP180 films, respectively. The work functions of all the samples were found to be higher than that of pure graphene due to the effect of oxidation and/or phosphor embedding. Generally, the oxidation of graphene results in an increase in hole concentration in GO, and thus work function increases. It is observed, from the XPS and XRD analyses, that the degree of oxidation is higher in GO70 film compared to GO180, GP70, and GP180 films. Therefore, the work function of the GO70 film is higher than that of the GO180, GP70, and GP180 films.[22]

The highest occupied molecular orbital (HOMO) values of the GO70, GO180, GP70, and GP180 films with respect to E_F were calculated from Figure 2d and are shown schematically in Figure 2f. For this calculation, the spectrum was calibrated with

DOI: 10.1021/am507342w
ACS Appl. Mater. Interfaces 2015, 7, 5693−5700

respect to the reference values of graphene (work function of 4.1 eV). The HOMO levels were shifted by 1.65, 0.9, 2.1, and 1.9 eV downward with respect to E_F for the GO70, GO180, GP70, and GP180 films, respectively.

The HOMO and the lowest unoccupied molecular orbital (LUMO) of graphene cross at the Dirac point, which results in zero bandgap. However, in GO70, bonding between the π and oxygen states produces electron transfer from graphene to oxygen; consequently, the HOMO state shifts downward from the Dirac point of pure graphene, which leads to gap opening. In the GO70 and GP70 films, bonding between the π and oxygen states leads to electron transfer from carbon to oxygen. As a result, the HOMO states in GO70 and GP70 were shifted downward from the Dirac point by 1.65 and 2.1 eV, respectively. A downward shift of 0.9 eV was observed in the GO180 film, which was lower than that in GO70, which is due to the partial restoration of the sp^2 clusters via annealing. The downward shift of 1.9 eV in the GP180 film was less than that in GP70, which again resulted from higher temperature annealing. The ionization potentials (calculated from Figure 2c,d) were 7.85, 6.7, 7.6, and 7.2 eV for the GO70, GO180, GP70, and GP180 films, respectively. Table 2 shows the values of the downward shift of HOMO from E_F, the work function, and the ionization potential of the films calculated from Figure 2d,e.

Table 2. Ionization Potential and Work Function Values of the Films, Calculated from Figure 2

sample	ref graphene	GO	GO180	GP	GP180
downward shift of HOMO from E_F (eV)		1.65	0.9	2.1	1.9
work function (eV)	4.1	6.2	5.8	5.5	5.3
ionization potential (eV)		7.85	6.7	7.6	7.2

The bandgap values of the films (which give rise to PL emission in the blue region) were measured using cyclic voltammetry (see Supplementary Information, Figure S2) and UPS spectra. Figure 3a schematically represents the E_{HOMO}, E_{LUMO}, and calculated band-gap values of the films. The band-gap values were found to be 2.05, 1.3, 2.56, and 2.43 eV for the GO70, GO180, GP70, and GP180 films, respectively. On the basis of the XPS, XRD, XAS, and CV analyses of our films, the PL emission from the GO70, GO180, GP70, and GP180 films are schematically illustrated as shown in Figure 3c. It can be concluded that C−N bonding, as observed from the XPS spectra, resulted in the emission at ~400 nm in the GP70 and GP180 films. The lone pair (LP) of electrons in the sp^2 C−N bond, which is not hybridized with the carbon and located in the π valence band (represented as LP in Figure 3c), is responsible for this emission.[23] This LP of electrons creates an energy level below the π band, and the transition from different π^* states to LP level results in the emission at ~400 nm.

The quantum yields of the emissions from the GO70, GO180, GP70, and GP180 films were 0.2, 0.2, 7.0, and 9.6%, respectively. The quantum yields of the GP70 and GP180 films are 35 times and 48 times higher than those of the GO70 and GO180 films, respectively. The phosphor embedding in the GO sheets enhanced their quantum yields. A further enhancement of the PL quantum yield in GP180 compared to that of GP70 was the result of the higher percentage of C−N bonding in the GO−phosphor nanoscrolls as observed by XPS analysis. Highly luminescent GO−phosphor hybrids with a high quantum yield may open important applications in the fabrication of graphene-based optoelectronic devices.

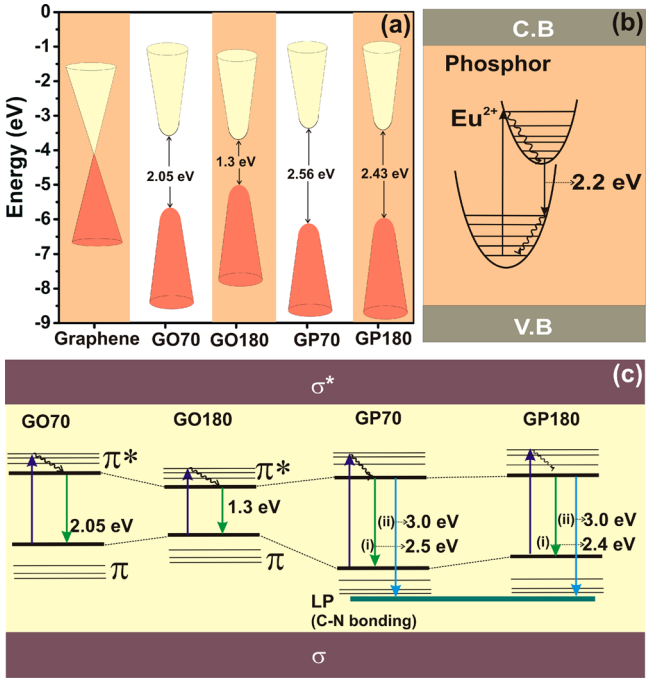

Figure 3. (a) Schematic representation of E_{HOMO}, E_{LUMO}, and band-gap values of the films measured through CV and UPS spectra, (b) schematic of PL emission from the phosphor, and (c) schematic of PL emission from GO70, GO180, GP70, and GP180 films.

The surface morphology and the structure of the GO and GP films were analyzed by using SEM images. The images of the GO70 and GO180 films exhibit a typical GO morphology with some wrinkles on the surface as shown in Figure 4a,b.

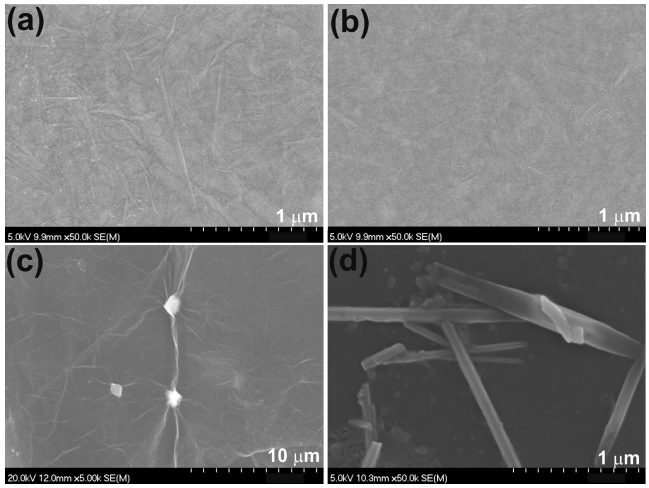

Figure 4. SEM images of (a) G070, (b) GO180, (c) GP70, and (d) GP180 films.

The morphology of the GP70 film (Figure 4c) shows that the GO sheets are about to scroll, while that of to the GP180 film exhibit perfect scrolls (Figure 4d). The edges of GO layer in GP180 film are folded back, scrolled into a tubular structure, and result in GONS due to the embedded phosphor. A size distribution analysis revealed that the scrolls had an average length of ~2 μm. Upon sonication of the GO−phosphor

DOI: 10.1021/am507342w
ACS Appl. Mater. Interfaces 2015, 7, 5693−5700

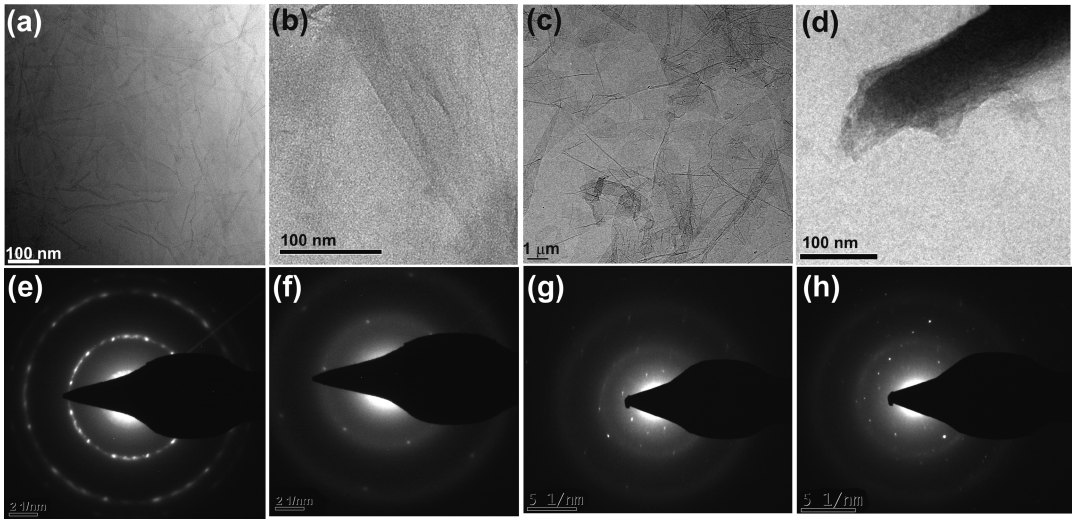

Figure 5. (a–d) The HRTEM images and (e–h) the corresponding SAED patterns of GO70, GO180, GP70, and GP180 films.

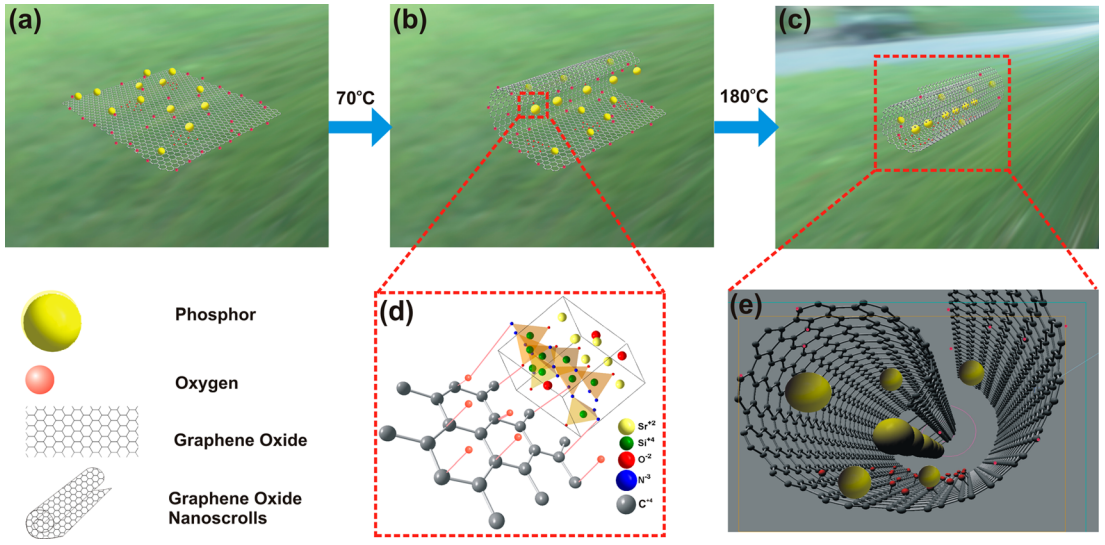

Figure 6. Schematic diagram showing (a) phosphor particles attached to GO sheets, (b) the GO sheets just beginning to scroll, (c) GO sheets completely scrolled at 180 °C, (d) the bonding between GO and phosphor, and (e) three-dimensional view of a single GO–phosphor scroll.

hybrids in water, the phosphor particles are attached to the GO film and spontaneously bend the GO sheets. Scrolling occurs because phosphor molecules embedded on the GO sheets make its planar structure extremely unfavorable to maintain.[24] The large GO sheets rapidly roll up and form entangled structures because the phosphor attachments prevent them from maintaining the high aspect ratio of the two-dimensional (2D) structure. The van der Waals attraction and the $\pi-\pi$ stacking effect between graphene layers play an important role in the scrolling phenomenon. Thus, via scrolling, the GO layer can overcome the energy barrier and fully wrap phosphor molecules. The GO70 and GO180 films did not exhibit any scrolling. However, the GO sheets in GP70 just began to scroll, indicating the role of phosphor embedding in the scrolling process (Figure 4c). The GP180 films exhibited a complete scroll formation, and the density of the scrolls was higher.

Figure 5a–d provides high-resolution transmission electron microscopy (HRTEM) images, and Figure 5e–h shows the corresponding SAED patterns of the GO70, GO180, GP70, and GP180 films, respectively. The TEM image and corresponding SAED pattern of the GO180 film exhibit typical sharp hexagonal spots and a lattice spacing of 0.76 nm, which have been identified as the (002) reflections of graphene lattice.[25]

The SAED pattern of the GP70 film in Figure 5g exhibits a mixed pattern of GO and carbon nanotube (CNT). Even though the pattern is closer to that of GO, it does not exactly match with those of pure GO or CNT. The SAED pattern in Figure 5h reveals that the lattice structure of the tubular scrolls is similar to that of CNTs and shows the presence of 00.2 and 00.4 reflections.[26] The lattice parameters measured from the corresponding SAED pattern in Figure 5h were consistent with the reported values of CNTs. More TEM images of the GP180 film are presented in Supplementary Information, Figure S3. On the basis of the SEM, TEM, and SAED analyses, the scroll formation process is schematically represented in Figure 6.

The Raman analysis of all the films show spectral features of graphene, exhibiting a G peak at ~1590 cm^{-1}, a D peak at ~1350 cm^{-1}, and a 2D peak at ~2697 cm^{-1} as shown in Figure 7.[27] The peak positions and full-width at half-maximum (fwhm,

DOI: 10.1021/am507342w
ACS Appl. Mater. Interfaces 2015, 7, 5693–5700

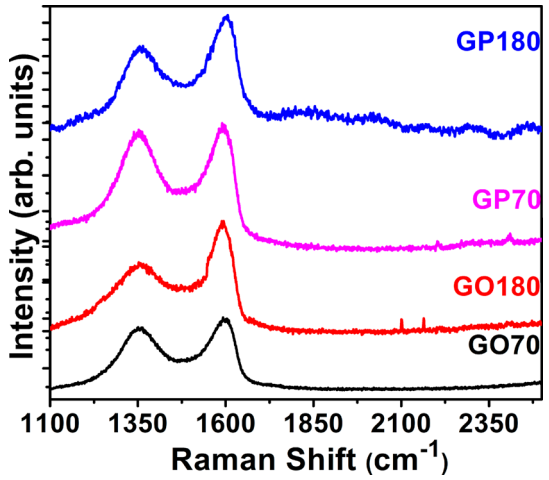

Figure 7. Raman spectra of GO70, GO180, GP70, and GP180 films.

G peak) are listed in Table 3. The D peak corresponds to disordered sp^2 carbon induced by the linking with sp^3 carbon atoms (in-plane carbon breathing mode (A_{1g} mode)), which is forbidden in defect free/perfect graphite.

Table 3. D Peak Position, G Peak Position, and the Corresponding G Peak FWHM Values in GO and GP Films

sample	D peak (cm^{-1})	G peak (cm^{-1})	fwhm (G peak) (cm^{-1})
GO70	1356	1592	75
GO180	1357	1590	63
GP70	1349	1598	84
GP180	1363	1607	78

Since the D peak depends on the oxygen content in GO, the shift of the D peak position in various films can be related to the variations in oxygen functionalities in the films. The G peak corresponds to graphite-like sp^2 carbon, which is a degenerate optical phonon mode at the Brillouin zone center and is induced by a single resonance process. The fwhm of G peak is a measure of disorder, and it increases continuously as the disorder increases.[28] The G peak fwhm value of GP70 film is bigger than that of the GO180 film, which indicates that the disorder in the GP70 film is greater than that in the GO180 film. Note that the G peaks of GP70 and GP180 films were shifted to a higher frequency compared with GO70 and GO180 films. The bonding between GO and the phosphor can alter the electronic properties of the GO–phosphor hybrid, resulting in the observed shifts of the G peak in GP70 and GP180 films.

4. CONCLUSIONS

An easy chemical route was chosen to prepare highly luminescent GO–phosphor hybrids and nanoscrolls. The GO nanoscrolls having tubular-like structures were prepared by wrapping phosphor molecules with GO sheets. The GO–phosphor hybrids exhibited a highly intense luminescence emission at ~537 nm. C–N bonding resulted in an additional broad luminescent emission at 400 nm. Our GO–phosphor hybrids demonstrated a maximum quantum yield of 9.6%, 48 times higher than that of pure GO. HRTEM images of the GP180 exhibited a well-defined tubular scroll, and the lattice planes calculated from the SAED pattern revealed CNT-like structural ordering. The SAED pattern of the GP70 film exhibited a mixed pattern of GO and CNTs, similar to the pattern of GO. X-ray diffraction and absorption spectra analyses revealed that the GO maintained its π–π^* absorption properties. This study demonstrated the fabrication of GO–phosphor nanoscrolls with a higher bandgap and strong luminescent emission in the violet and green regions. The synthesized GO–phosphor nanoscrolls are expected to have promising applications in optoelectronic devices.

■ ASSOCIATED CONTENT

Supporting Information

Si 2p and O 1s XPS spectra of GO and GP films. Cyclic voltammetry curves of GO and GP films. HRTEM images of GP180 films. UV–visible absorption spectra of GO and GP films. This material is available free of charge via the Internet at http://pubs.acs.org.

■ AUTHOR INFORMATION

Corresponding Author

*E-mail: jjang@gist.ac.kr.

Author Contributions

The manuscript was written through contributions of all authors. All authors have given approval to the final version of the manuscript.

Notes

The authors declare no competing financial interest.

■ ACKNOWLEDGMENTS

This work was supported by the National Leading Research Lab Program (Grant No. 2013035351) funded by the National Research Foundation of Korea and by the Core Technology Development Program for Next-Generation Solar Cells of the Research Institute for Solar and Sustainable Energies (RISE), GIST.

■ ABBREVIATIONS

GO, graphene oxide
GONS, graphene oxide nanoscrolls

■ REFERENCES

(1) Geim, A. K.; Novoselov, K. S. The Rise of Graphene. *Nat. Mater.* **2007**, *6*, 183–191.
(2) Novoselov, K. S.; Geim, A. K.; Morozov, S. V.; Jiang, D.; Katsnelson, M. I.; Grigorieva, I. V.; Dubonos, S. V.; Firsov, A. A. Two-Dimensional Gas of Massless Dirac Fermions in Graphene. *Nature* **2005**, *438*, 197–200.
(3) Wang, X.; Zhi, L.; Müllen, K. Transparent, Conductive Graphene Electrodes for Dye-Sensitized Solar Cells. *Nano Lett.* **2007**, *8*, 323–327.
(4) Baskey, M.; Saha, S. K. A Graphite-Like Zero Gap Semiconductor with an Interlayer Separation of 2.8 Å. *Adv. Mater.* **2012**, *24*, 1589–1593.
(5) Dikin, D. A.; Stankovich, S.; Zimney, E. J.; Piner, R. D.; Dommett, G. H. B.; Evmenenko, G.; Nguyen, S. T.; Ruoff, R. S. Preparation and Characterization of Graphene Oxide Paper. *Nature* **2007**, *448*, 457–460.
(6) Eda, G.; Lin, Y.-Y.; Mattevi, C.; Yamaguchi, H.; Chen, H.-A.; Chen, I. S.; Chen, C.-W.; Chhowalla, M. Blue Photoluminescence from Chemically Derived Graphene Oxide. *Adv. Mater.* **2010**, *22*, 505–509.
(7) Gokus, T.; Nair, R. R.; Bonetti, A.; Böhmler, M.; Lombardo, A.; Novoselov, K. S.; Geim, A. K.; Ferrari, A. C.; Hartschuh, A. Making Graphene Luminescent by Oxygen Plasma Treatment. *ACS Nano* **2009**, *3*, 3963–3968.

DOI: 10.1021/am507342w
ACS Appl. Mater. Interfaces 2015, 7, 5693–5700

(8) Mei, Q.; Zhang, K.; Guan, G.; Liu, B.; Wang, S.; Zhang, Z. Highly Efficient Photoluminescent Graphene Oxide with Tunable Surface Properties. *Chem. Commun.* **2010**, *46*, 7319−7321.
(9) Shi, X.; Pugno, N. M.; Gao, H. Tunable Core Size of Carbon Nanoscrolls. *J. Comput. Theor. Nanosci.* **2010**, *7*, 517−521.
(10) Marcano, D. C.; Kosynkin, D. V.; Berlin, J. M.; Sinitskii, A.; Sun, Z.; Slesarev, A.; Alemany, L. B.; Lu, W.; Tour, J. M. Improved Synthesis of Graphene Oxide. *ACS Nano* **2010**, *4*, 4806−4814.
(11) Anoop, G.; Cho, I. H.; Suh, D. W.; Yoo, J. S. Luminescence Characteristics of $Sr_{1-x}Ba_xSi_2O_2N_2:Eu^{2+}$ Phosphors for White Light Emitting Diodes. Phys. *Status Solidi A* **2012**, *209*, 2635−2640.
(12) Cho, I. H.; Anoop, G.; Suh, D. W.; Lee, S. J.; Yoo, J. S. On the Stability and Reliability of $Sr_{1-x}Ba_xSi_2O_2N_2:Eu^{2+}$ Phosphors for White LED Applications. *Opt. Mater. Express* **2012**, *2*, 1292−1305.
(13) Rani, J. R.; Lim, J.; Oh, J.; Kim, J.-W.; Shin, H. S.; Kim, J. H.; Lee, S.; Jun, S. C. Epoxy to Carbonyl Group Conversion in Graphene Oxide Thin Films: Effect on Structural and Luminescent Characteristics. *J. Phys. Chem. C* **2012**, *116*, 19010−19017.
(14) Barr, T. L. An XPS Study of Si As It Occurs in Adsorbents, Catalysts, and Thin Films. *Appl. Surf. Sci.* **1983**, *15*, 1−35.
(15) Wu, S. L.; Cui, Z. D.; He, F.; Bai, Z. Q.; Zhu, S. L.; Yang, X. J. Characterization of the Surface Film Formed from Carbon Dioxide Corrosion on N80 Steel. *Mater. Lett.* **2004**, *58*, 1076−1081.
(16) Gulbagh, S.; Sutar, D. S.; Botcha, V. D.; Pavan, K. N.; Talwar, S. S.; Srinivasa, R. S.; Major, S. S. Study of Simultaneous Reduction and Nitrogen Doping of Graphene Oxide Langmuir−Blodgett Monolayer Sheets by Ammonia Plasma Treatment. *Nanotechnology* **2013**, *24*, 355704.
(17) Wang, P.; Wang, Z.; Jia, L.; Xiao, Z. Origin of the Catalytic Activity of Graphite Nitride for the Electrochemical Reduction of Oxygen: Geometric Factors Vs. Electronic Factors. *Phys. Chem. Chem. Phys.* **2009**, *11*, 2730−2740.
(18) Kovac, B.; Ljubic, I.; Kivimaki, A.; Coreno, M.; Novak, I. Characterisation of the Electronic Structure of Some Stable Nitroxyl Radicals Using Variable Energy Photoelectron Spectroscopy. *Phys. Chem. Chem. Phys.* **2014**, *16*, 10734−10742.
(19) Nethravathi, C.; Rajamathi, M. Chemically Modified Graphene Sheets Produced by the Solvothermal Reduction of Colloidal Dispersions of Graphite Oxide. *Carbon* **2008**, *46*, 1994−1998.
(20) Zhao, J. P.; Chen, Z. Y.; Yano, T.; Ooie, T.; Yoneda, M.; Sakakibara, J. Core-Level and Valence-Band Characteristics of Carbon Nitride films with High Nitrogen Content. *Appl. Phys. A: Mater. Sci. Process.* **2001**, *73*, 97−101.
(21) Hae Kyung, J.; Cheolsoo, Y.; Bong Soo, K.; Ki-jeong, K. Valence Band of Graphite Oxide. *Europhys. Lett.* **2010**, *92*, 37005.
(22) Lee, D. H.; Lee, J. A.; Lee, W. J.; Kim, S. O. Flexible Field Emission of Nitrogen-Doped Carbon Nanotubes/Reduced Graphene Hybrid Films. *Small* **2011**, *7*, 95−100.
(23) Zhang, Y.; Pan, Q.; Chai, G.; Liang, M.; Dong, G.; Zhang, Q.; Qiu, J. Synthesis and Luminescence Mechanism of Multicolor-Emitting γ-C_3N_4 Nanopowders by Low Temperature Thermal Condensation of Melamine. *Sci. Rep.* **2013**, *3*, 1943.
(24) Sharifi, T.; Gracia-Espino, E.; Reza Barzegar, H.; Jia, X.; Nitze, F.; Hu, G.; Nordblad, P.; Tai, C.-W.; Wågberg, T. Formation of Nitrogen-Doped Graphene Nanoscrolls by Adsorption of Magnetic γ-Fe_2O_3 Nanoparticles. *Nat. Commun.* **2013**, *4*, 2319.
(25) Rani, J. R.; Oh, J.; Park, J.-e.; Lim, J.; Park, B.; Kim, K.; Kim, S.-J.; Chan Jun, S. Controlling the Luminescence Emission From Palladium Grafted Graphene Oxide Thin Films via Reduction. *Nanoscale* **2013**, *5*, 5620−5627.
(26) Kumar, R.; Tiwari, R. S.; Srivastava, O. N. Scalable Synthesis of Aligned Carbon Nanotubes Bundles Using Green Natural Precursor: Neem Oil. *Nanoscale Res. Lett.* **2011**, *6*, 92.
(27) Graf, D.; Molitor, F.; Ensslin, K.; Stampfer, C.; Jungen, A.; Hierold, C.; Wirtz, L. Spatially Resolved Raman Spectroscopy of Single- and Few-Layer Graphene. *Nano Lett.* **2007**, *7*, 238−242.
(28) Ferrari, A. C.; Robertson, J. Interpretation of Raman Spectra of Disordered and Amorphous Carbon. *Phys. Rev. B* **2000**, *61*, 14095−14107.

DOI: 10.1021/am507342w
ACS Appl. Mater. Interfaces 2015, 7, 5693−5700